X-rays, -rays, electrons and protons radiation-induced changes on the lifetimes of Er3+and Yb3+ions in silica-based optical fibers

X-rays, γ-rays, electrons and protons radiation-induced changes on the lifetimes of Er^{3+} and Yb^{3+} ions in silica-based optical fibers

Ayoub Ladaci[1,2,3,*], Sylvain Girard[1], Luciano Mescia[2], Thierry Robin[3], Arnaud Laurent[3], Benoit Cadier[3], Mathieu Boutillier[4], Adriana Morana[1], Diego Di Francesca[1], Youcef Ouerdane[1] and Aziz Boukenter[1]

[1]Univ Lyon, Laboratoire Hubert Curien UMR CNRS 5516,18 Rue Pr Benoît Lauras, 42000 Saint-Étienne, France

[2]Politecnico di Bari, Via Amendola, 126/B, 70126 Bari, Italy

[3]iXBlue Photonics, Rue Paul Sabatier. 22300, Lannion, France

[4]Centre National d'Études Spatiales, CNES 18 Av Edouard Belin, 31400 Toulouse, France

Abstract

The evolution of Ytterbium $^2F_{5/2}$ and Erbium $^4I_{13/2}$ energy level lifetimes with various types of radiation (40 keV X-rays, 480 MeV protons, 1.2 MeV γ-rays and 6 MeV electrons) were investigated on samples of silica-based Rare-Earth Doped optical Fibers (REDFs). For each studied sample (Er-doped and Er/Yb-doped), a strong dependence of the lifetime value on the irradiation dose (for equivalent doses ranging from 10 $Gy(SiO_2)$ to 10 $MGy(SiO_2)$) is observed regardless of the nature of the radiation. For both types of fibers and ions, complex dose dependences are observed: a limited decrease of the lifetime at the lower doses, whereas a large reduction is reported at doses exceeding 100 $kGy(SiO_2)$. The results allow to estimate the vulnerability of REDF based systems, such as optical amplifiers and sources, for space and nuclear applications. In such harsh environments, Radiation Induced Attenuation (RIA) is also a key issue. The positive and stabilizing effect of Ce co-doping on both the RIA and the lifetimes is reported even at the highest dose of 10 $MGy(SiO_2)$. The basic mechanisms involved during the interaction between radiation and fiber material were also investigated through low temperature spectroscopic measurements that revealed the fundamental role of radiation-induced point defects.

1 INTRODUCTION

During the past decades, Rare Earth Doped Fiber Amplifiers (REDFAs) widely increased the performances of telecommunications systems, particularly in terms of long-distance transmission [1]. These optical amplifiers are based on active single-mode optical fibers having their cores doped with Rare Earth (RE) ions such as Er^{3+}, Yb^{3+} or combination of both of them. Moreover, REDFA or RE-Doped Fiber Sources (REDFS) technologies are nowadays mature and routinely employed

thanks to effective and reliable characteristics such as high gain, high output power, polarization independent gain, absence of crosstalk, low noise figure, and low insertion loss [2-5].

Since 90's, the REDFA's and REDFS's systems were also considered for integration in spacecrafts as part of high speed data links (EDFAs or EYDFAs), fiber-optic gyroscope (Er or Er/Yb-EDFSs) or deep-space optical communication (Yb-EDFS). Despite the many advantages, their integration is still limited by the impact of space harsh radiation constraints (protons, electrons, heavy ions…) on their performances, mainly through a degradation of the active transmission properties [6]. Radiation affects the REDFs mainly through the radiation-induced attenuation (RIA) caused by point defects created in the host silica matrix predominantly by ionization processes [7]. Most of the previous studies focused on space needs with limited dose of radiation, few tens of Gy(SiO_2) [8,9]. However, for future mission, such as the ones to Jupiter's moons, the total dose levels are expected to increase with a stronger contribution of electron radiation. Furthermore, prospective studies regarding the use of high power fiber laser for nuclear industry, e.g. for dismantling applications, are today under progress. For these last applications, higher dose levels, such as multi-MGy of γ-rays, are expected. RIA in RE-doped fibers seems caused by point defects related to the co-dopants such as phosphorus or/and aluminum that are added into the silica-based host matrix to optimize the RE incorporation, limiting the clustering and then enhancing the amplification efficiency [10]. To mitigate the RIA and improve the hardness levels of REDFs, several approaches were proposed. Among the most effective ones, one can cite Cerium codoping and H_2 or D_2 loading [11,12]. Both approaches reduce the concentrations of P or Al-related defects and then decrease the RIA impacting the fiber-based device performance. Another technique is based on an alternative manufacturing process allowing to incorporate the RE ions into the a-SiO_2 while keeping low the P or Al concentrations [13] and the associated radiation induced absorption bands at thepump (~ 980 nm) and signal (~ 1550 nm) wavelengths [14]. In addition to the RIA, radiation induced point defects which are created in proximity of RE ions are expected to change their spectroscopic properties of the latters. Indeed, it was demonstrated in [15] that luminescence lifetimes of both

Erbium and Ytterbium ions embedded in complex bulk materials designed for nuclear waste management strongly decrease when these glasses are irradiated at the extreme dose levels (~10^9 Gy) associated with these applications.

Another active research field concerns the modeling of REDFAs performance during a space mission. Numerical codes are today developed to predict the vulnerability of a given EDFA architecture for a mission profile [16]. These tools consider only the RIA impact on the gain and noise figure as RIA is clearly the dominant damage mechanism [17, 18, 19]. However, the consideration of further degradation mechanisms, as those related to changes in the spectroscopic parameters of RE ions, will open the way to even more accurate predictions in a larger range of doses. In [20], a parametric and systematic (±20 %) evaluation of the possible impact of a change of these parameters on the gain of an EDFA was provided, allowing to identify the most 11. In the present work, we acquired the needed experimental data to investigate the changes of RE ion lifetimes under irradiation and extended the dose range and the natures of particles to cover the whole spectrum of possible harsh environments of interest for REDFs.

We investigated the evolution of the Erbium $^4I_{13/2}$ and the Ytterbium $^2F_{5/2}$ energy levels lifetime in phosphosilicate fibers, representative of the state-of-the-art commercial REDFs, from low doses (10 Gy) up to MGy levels. Moreover, this investigation was also performed on an Erbium/Cerium codoped sample, being one of the most radiation resistant fiber ever reported [21] to check if the Ce also helps preserving the optical ion properties in addition to reducing the RIA [11]. Finally, low temperature measurements and spectroscopic analyses have also been carried out to improve our understanding of the different basic mechanisms taking place in irradiated silica-based optical fibers.

2 EXPERIMENTAL DETAILS

2.1 Tested samples

A dedicated set of single mode (at 1550 nm) phosphosilicate optical fibers with octagonal double clad geometry were manufactured by iXBlue [22]. Samples PYb and PYbEr are Yb^{3+} and Er^{3+}/Yb^{3+} co-doped, respectively. PYbErCe sample is co-doped with Er^{3+}/Yb^{3+} and Ce^{3+}. Table I summarizes the main characteristics of each sample.

Table I: Main characteristics of tested samples

Sample	[P] (wt. %)	[Yb] (wt. %)	[Er] (wt. %)	[Ce] (wt. %)	Core diameter (μm)	Outer cladding diameter (μm)
PYb	8.7	3.3	-	-	8.3	125
PYbEr	8.8	3.5	0.08	-	12.9	125
PYbErCe	12.1	1.5	0.07	~0.6	6	135

2.2 Irradiation facilities and experimental procedure

Several facilities were used to cover the variety of radiation fields: X-rays, protons, γ-rays and electrons. For the X-rays, tests were performed using the MOPERIX X-ray facility from Hubert Curien (France) : 40 keV mean photon energy and dose rate ranging from 3.6 to 180 kGy(SiO_2)/h. Proton irradiation was performed at the PIF facility from TRIUMF laboratories (Vancouver, Canada) with protons of 480 MeV energy. Gamma irradiations were performed using ^{60}Co sources having energy of 1.2 MeV. For low doses [30-300 kGy] the irradiation was performed at the IRMA facility of IRSN Institute (Saclay, France) using a dose rate between 0.2 and 2 kGy/h whereas higher doses [0.3-10 MGy] were carried out at the BRIGITTE facility of SCK-CEN (Mol, Belgium) using dose rates ranging between 10 and 30 kGy/h. Electron irradiations were carried out at CEA DAM center of Gramat (France) with the ORIATRON facility delivering electrons with energy of ~6 MeV at dose rate ranging from 0.7 to 1.3 kGy/min. All these irradiations were executed at room temperature between 20 and 35°C. All the reported measurements were performed more than 3 days after the end of these irradiations, meaning that our study is limited to the permanent radiation-

induced changes. The transient effects that occur during irradiation and that immediately recover when the irradiation ends were not investigated.

2.3 Lifetime measurements

A dedicated Time Resolved Luminescence (TRL) setup was used for the lifetime measurements. The system is pumped by a pulsed Nd-YAG laser, delivering 5 ns long pulses at 1064 nm with a repetition rate of 10 Hz. The pump is feeded into an optical parametric oscillator and second harmonic generator to give a tunable wavelength laser range between 216 nm and 2µm (GWU Lasertechnik). The time dependence of the luminescence spectrum of the Er^{3+} ions (due to the transition $^4I_{13/2} \rightarrow {}^4I_{15/2}$ at ~ 1550 nm) was recorded using an externally triggered ANDOR infrared (IR) spectrometer. While, the time dependence of the luminescence spectrum of Yb^{3+} ions (due to the transition $^2F_{5/2} \rightarrow {}^2F_{7/2}$ at ~ 980 nm) was analyzed using a photomultiplier coupled to an Agilent 7000B 500 MHz oscilloscope (Fig. 1.a). The low temperature measurements were recorded by sinking the optical fiber samples in a liquid nitrogen bath. The sample under test is spliced at its two ends with two passive multi-mode optical fibers allowing to inject the excitation laser pulse into the sample and to deliver the collected luminescence to the spectrometer (Fig. 1.b).

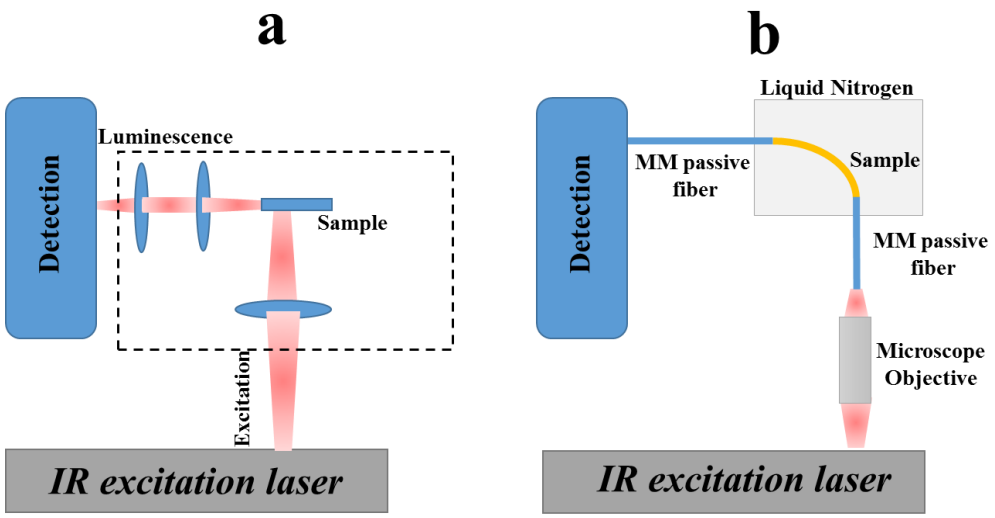

Fig. 1: Setup for the time resolved luminescence experiments a) Room-Temperature (RT) configuration b) Low-Temperature (LT) configuration

It was established that in an amorphous silica glass, the RE ions lifetime decay follows a stretched experimental law as given in Equation 1 [23]:

$$f(t) = A_1 \exp\left(-t/\tau_1\right)^{\beta} \qquad (1)$$

where A_1 is the initial luminescence amplitude, t is the time after the excitation, τ_1 is the lifetime of the involved energy level and β is the stretching parameter. We then used this stretched experimental law to fit the luminescence decay as a function of the time and to extract the lifetime values, it was observed that $\beta = 0.98$ provides the best fits for all the luminescence decays.

2.3 In-Situ RIA Measurements

RIA measurements were performed *in situ* at RT by recording the fiber transmission infrared spectrum before, during and after the X-rays runs using a light source EQ99, from Energetic, and an Optical Spectrum Analyzer (OSA), from Yokogawa (see Fig. 2). We irradiated about 12 cm of RE-doped fiber spliced to two radiation hardened single mode fiber pigtails. The dose rate was set to ~9 Gy/s and the total accumulated dose was fixed to ~3 MGy(SiO_2).

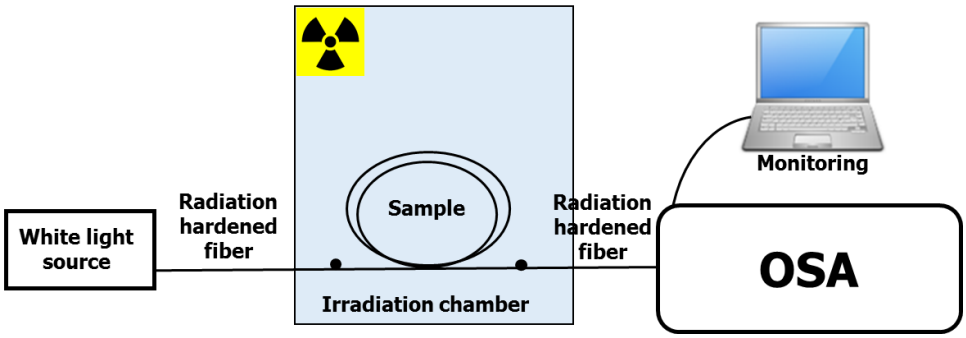

Fig. 2: Schematic setup used for the RIA measurements during and after irradiation.

3 RESULTS AND DISCUSSION

3.1 Lifetimes evolution with the irradiation dose

The investigation of the Yb^{3+} $^2F_{5/2}$ energy level lifetime dependence on the irradiation dose was done on the PYb samples irradiated at different doses and at different radiation facilities and under a 940 nm excitation waveltngth. A review of the whole set of results is reported in Fig. 3. The lifetime obviously decreases when the dose increases: two different behaviors can be clearly distinguished. In the non-irradiated sample (reference), the measured lifetime is about ~1.8 ms. In the first zone (up to 100 kGy), the lifetime tends to decrease linearly in a log-log scale down to the 0.65 ms value at 100 kGy. For higher doses (zone 2), the lifetime remains nearly unchanged.

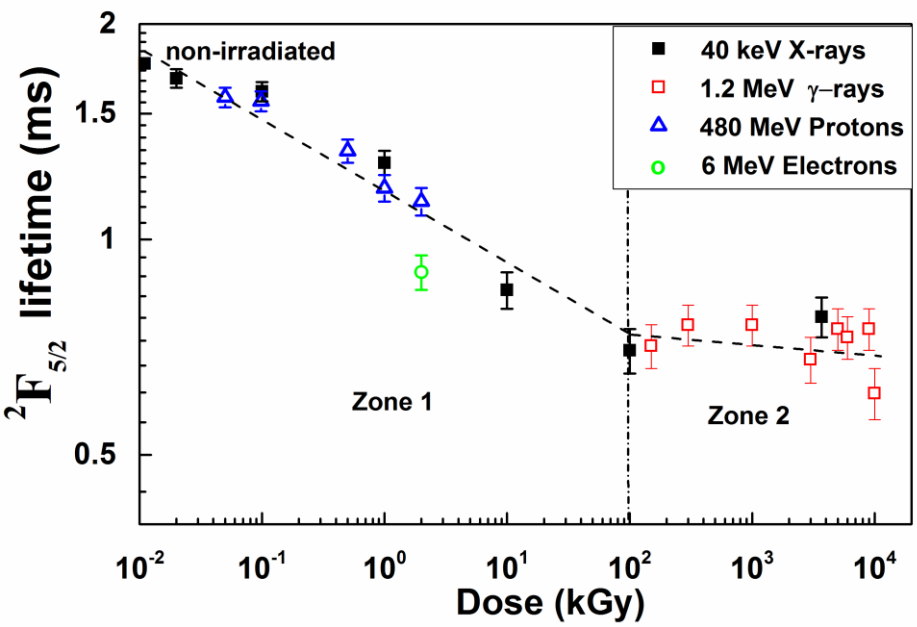

Fig. 3: Equivalent Dose dependence of the $^2F_{5/2}$ energy level lifetime of PYb samples irradiated with X-rays, γ-rays, protons and electrons

The luminescence lifetime of the Er^{3+} $^4I_{13/2}$ energy level was investigated under 976 nm laser excitation. In particular, its evolution with the deposited dose was studied using the samples of PYbEr irradiated in the various radiation facilities. The obtained results are shown in Fig. 4. In this case, three different behaviors (zones) can be easily distinguished. In zone 1 (up to 100 kGy), we also measure a linear decrease (in a log-log scale) of the luminescence lifetime from ~ 9ms (non-irradiated sample) down to ~7.5 ms at 100 kGy. Between 100 kGy and 3 MGy, the lifetime remains mostly unchanged, around 7.5 ms (zone 2). For doses exceeding 3 MGy, the lifetime starts again to decrease following another linear curve (log-log) characterized by a higher slope (zone 3).

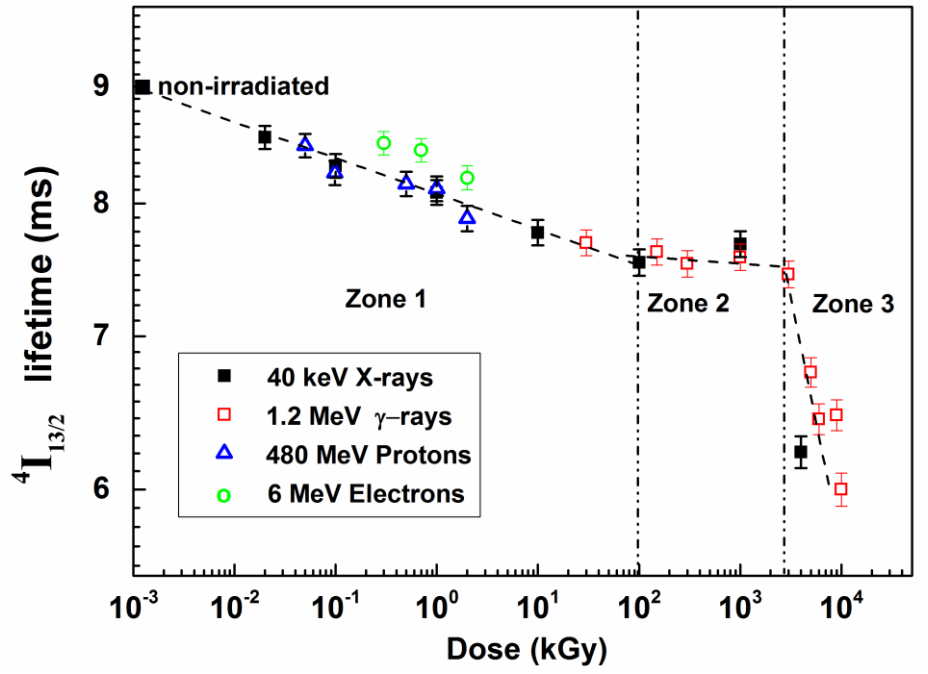

Fig. 4: Equivalent Dose dependence of the $^4I_{13/2}$ energy level lifetime of PYbEr samples irradiated with X-rays, γ-rays, protons and electrons

It is important to notice that similar lifetime evolutions are observed for the very different types of irradiations for both Er^{3+} $^4I_{13/2}$ and Yb^{3+} $^2F_{5/2}$ energy levels. This result highlights that, in first approximation, the RE lifetime is similarly affected by all types of radiation at equivalent doses. This is in agreement with the previous results regarding the RIA after γ-rays and proton exposures, and supporting ionization processes at the main origin of this radiation-induced effect [24, 25].

To investigate the Ce^{3+} co-doping influence on the radiation effects on Erbium lifetime, the X and γ-rays irradiated samples of PYbErCe fiber were studied and the lifetimes of the Erbium $^4I_{13/2}$ energy level extracted. All obtained results are reported in Fig. 5.

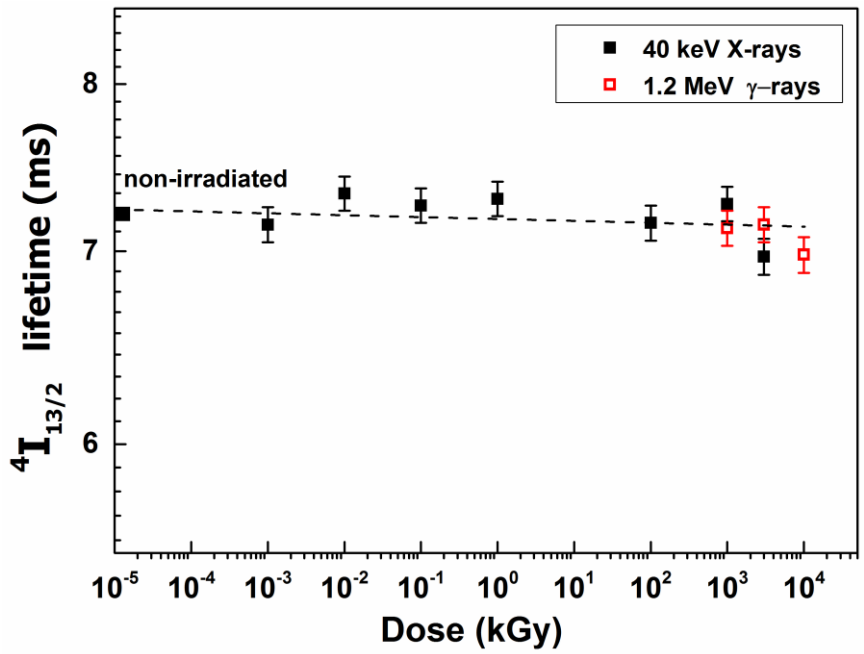

Fig. 5: Dose dependence of the Lifetime of the $^4I_{13/2}$ energy level lifetime of PYbErCe samples irradiated with X-rays and γ-rays.

For this Ce-codoped fiber, the erbium lifetime remains almost unaffected by irradiation. From our results, we observe a slight decrease from 7.2 ms (non-irradiated sample) to 6.9 ms (for a cumulated dose of 10 MGy) while the lifetime of the Ce free sample decreases from 9 ms to 6.9 ms under the same test conditions. Cerium is known to act as a matrix stabilizer that allows the manufacturing of radiation hardened Er^{3+}-doped and Er^{3+}/Yb^{3+}-codoped fibers [26, 27]. Fig. 6 illustrates the

normalized Erbium infrared luminescence spectra of both non-irradiated and 10 MGy irradiated samples of PYbEr and PYbErCe fibers.

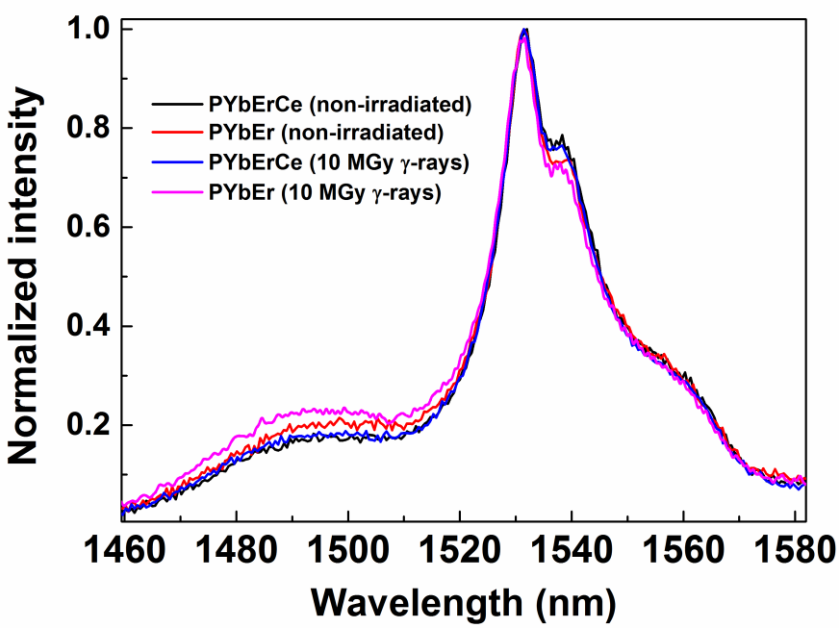

Fig. 6: Normalized luminescence of the Er^{3+} $^4I_{13/2}$ energy level with 976 nm pumping wavelength for both PYbErCe and PYbEr samples, non-irradiated and irradiated with γ-rays at 10 MGy dose level.

The Er^{3+} infrared normalized emission spectra have similar shapes in both samples (with and without Ce^{3+}), and this spectral shape remains mostly preserved even after 10 MGy dose.

3.2 RIA evolution during the irradiation

It is interesting to characterize the dose dependence of the RIA at ~ 1550 nm during the irradiation (Fig. 7). Under irradiation, a large number of defects are created in the phosphosilicate host matrix of both PYbEr and PYbErCe samples. Due to Ce codoping, there is a decrease of the IR absorbing species (mainly P1-defects [14]) in the Ce-doped sample [27] resulting in lower RIA level and different growth kinetics than those observed for the Ce-free sample. For this last class of samples, two kinetics for the RIA growth are present that seem compatible with the zones observed investigating the lifetimes in this fiber. The results were obtained in very different configurations: online for the RIA and post mortem for the lifetime. Nevertheless, for what concerns the IR

absorption band of P1 defect, it is known that these active centers are stable at room temperature allowing to compare the results obtained during and after the irradiation for this particular defect [28, 29, 30]. Figure 7.b represents the RIA in the infrared spectral domain where we observe the P_1 related absorption band responsible of the attenuation around 1550 nm and the Phosphorus Oxygen Hole Centers (POHC) tail which induce the RIA around 980 nm [14]. Despite this, a considerable RIA level is generated in the matrix even with the presence of Ce in the glass. However, the Ce ions stabilize the Er^{3+} spectroscopic parameters during the irradiation preserving a constant value of the lifetime even at very high irradiation doses.

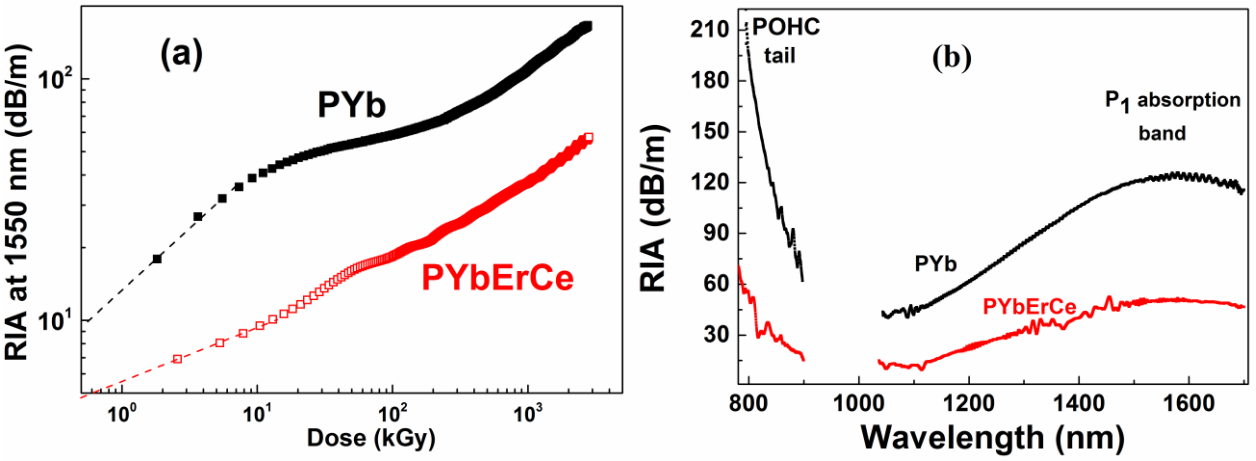

Fig. 7: RIA measurement on PYb and PYbErCe samples; (a) 1550 nm RIA growth dependence with dose during exposure to X-rays. (b) RIA spectra measured at the end of the X-ray irradiation at ~ 3 MGy

3.3 Low-Temperature lifetime measurements

Low-Temperature (LT, at 77 K) lifetime measurements have been performed in order to investigate the behaviors of Erbium ions with and without Ce^{3+} ion presence. Fig. 8 compares for both PYbEr and PYbErCe samples the normalized $^4I_{13/2}$ Er^{3+} luminescence decays measured under the same conditions at RT (300 K) and LT (77 K) for both pristine and irradiated samples.

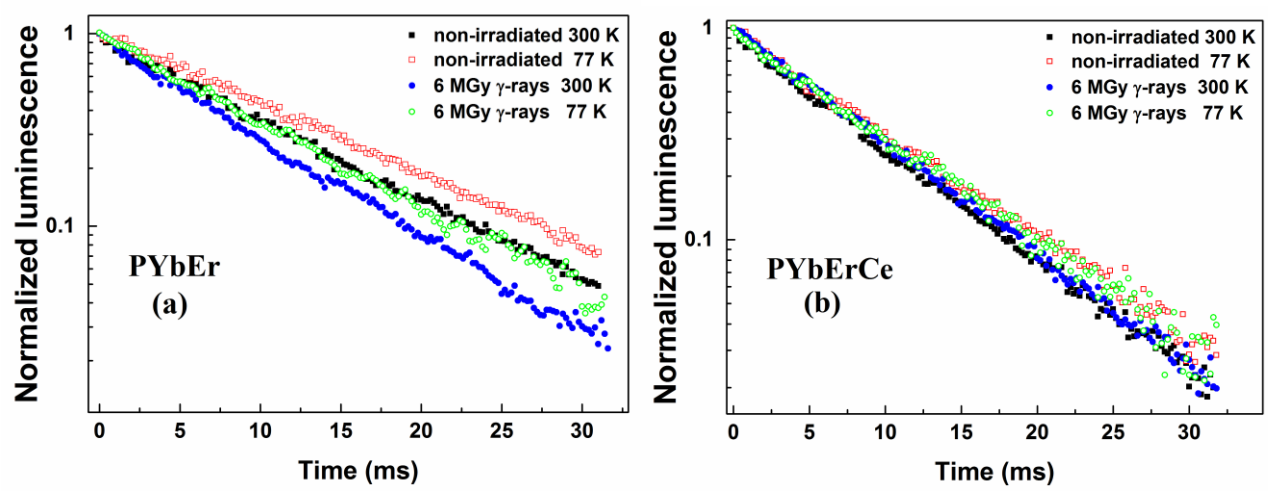

Fig. 8: Normalized luminescence decays of the $^4I_{13/2}$ Er^{3+}-energy level at RT and LT for non-irradiated and 6 MGy γ-ray irradiated samples (a) PYbEr and (b) PYbErCe.

These results show that the lifetime increases when decreasing the temperature in both non-irradiated and 6 MGy irradiated samples of PYbEr fiber. This behavior can be explained by the decrease of the non-radiative decay rate which directly impacts the lifetime of the $^4I_{13/2}$ Er^{3+}-energy level. However, in the case of the Ce-doped PYbErCe sample, the lifetime of this $^4I_{13/2}$ Er^{3+}-energy level in presence of Ce^{3+} ions (PYbErCe) seems less affected by temperature, providing again evidence that Cerium stabilizes the Er^{3+} $^4I_{13/2}$ energy level lifetime to temperature as it does for irradiation.

Fig. 9 compares the luminescence spectra at RT (300 K) and LT (77 K) temperatures. Lowering the temperature clearly changes the emission spectrum and this for the two investigated optical fibers. The emission bands become sharper because of the decrease of the line broadening mechanisms at 77 K. For PYbEr sample (Fig. 9.a) a larger diminution of the emission signal at low temperature occurs than in PYbErCe sample (Fig. 9.b). This behavior is caused by the reduction of the non-radiative $^4I_{11/2}\rightarrow{}^4I_{13/2}$ transition at LT which directly impacts the $^4I_{13/2}\rightarrow{}^4I_{15/2}$ transition. For PYbErCe sample the intensity is mostly preserved between RT and LT measurements. The presence

of Ce^{3+} ions triggers an energy transfer phenomenon which promotes the $^4I_{11/2} \rightarrow {}^4I_{13/2}$ non-radiative transition [31].

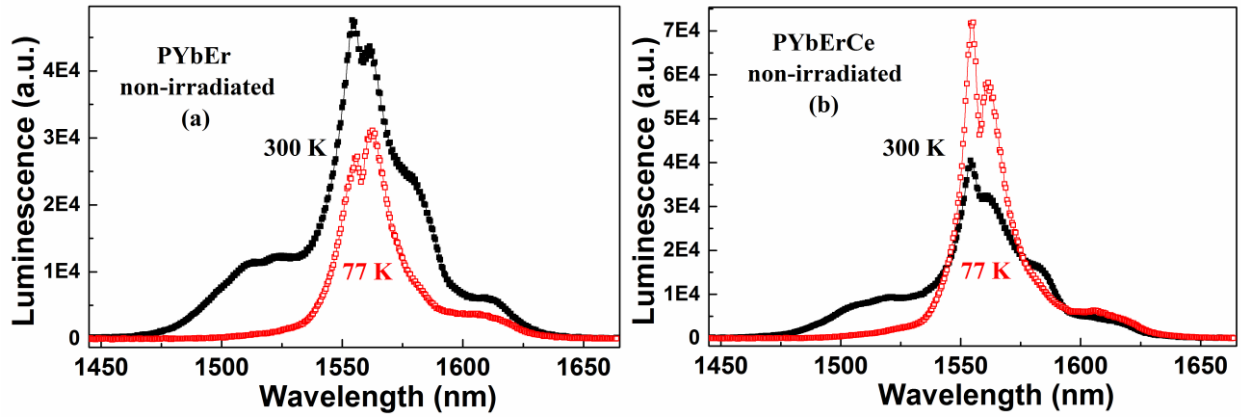

Fig. 9: Luminescence intensity spectra at RT (black squares) and LT (77 K, empty red squares) temperature (a) for PYbEr sample without Ce^{3+}-doping and (b) for PYbErCe sample with Ce^{3+}-doping.

4 CONCLUSION

We investigated the evolutions of the spectroscopic properties of Er^{3+} and Yb^{3+} ions embedded in a phosphosilicate fiber core silica-based matrix at different equivalent irradiation doses deposited by different particles such as X-rays, γ-rays, electrons and protons. We observed that for standard phosphosilicate matrix, the IR emission lifetimes of both ions strongly decrease, after irradiation, as a function of the dose, regardless of the type of radiation. A decrease from ~1.8 ms before irradiation to ~0.65 ms after 10 MGy is measured for the Yb^{3+} $^2F_{5/2}$ energy level and from ~9 ms to ~6.3 ms for the Er^{3+} $^4I_{13/2}$ energy level.

This investigation was also performed on radiation hardened Erbium-doped fiber containing Cerium ions to improve its tolerance to RIA effects. In addition to its positive impact on these excess losses, Cerium also reduces the impact of radiation on the Erbium lifetime. Additional low-temperature measurements provide evidence that the Cerium stabilizes the Er^{3+} $^4I_{13/2}$ energy level lifetime as a

function of the irradiation as well as for the temperature changes. A large lifetime evolution is observed in the Ce-free irradiated samples; these lifetime variations are associated with the very high RIA levels making their integration in REDFAs impossible in such conditions (dozens of dB/m after few kGy of irradiation). In the case of Ce-doped sample, the RIA level is lowered and the lifetime remains constant at the application doses. These results then illustrate the potential of Cerium-codoped RE-fibers to serve at higher dose environments, with limited RIA increase and almost no change in the RE ion properties.

REFERENCES

[1] V. Ter-Mikirtychev, Fundamentals of Fiber Lasers and Fiber Amplifiers, Springer, 2014.

[2] M.J.F. Digonnet, Rare-earth-doped fiber lasers and amplifiers, Marcel Dekker Inc. 2001.

[3] A. D'Orazio, M. De Sario, L. Mescia, V. Petruzzelli, Refinement of Er^{3+}-doped hole-assisted optical fiber amplifier, Opt. Express. 25 (2005) 9970-9981.

[4] B. Pedersen, K. Dybdal, C.D. Hansen, A. Bjarklev, J.H. Povlsen, H. Vendeltorp-Pommer, C.C. Larsen, Detailed theoretical and experimental investigation of high-gain erbium-doped fiber amplifier, IEEE Photon. Technol. Lett. 2 (1990) 863-865.

[5] M. De Sario, L. Mescia, F. Prudenzano, F. Smektala, F. Deseveday, V. Nazabal, J. Troles, L. Brilland, Feasibility of Er^{3+}-doped, $Ga_5Ge_{20}Sb_{10}S_{65}$ chalcogenide microstructured optical fiber amplifiers, OPT LASER TECHNOL. 41 (2009) 99-106.

[6] J.L. Barth, Space and Atmospheric Environments: From Low Earth Orbits to Deep Space, in: Protection of Materials and Structures from Space Environment: ICPMSE-6, Springer, Netherlands, 2003, pp.7-29.

[7] S. Girard, J. Kuhnhenn, A. Gusarov, B. Brichard, M.Van Uffelen,Y. Ouerdane, A. Boukenter, C. Marcandella, Radiation Effects on Silica-Based Optical Fibers: Recent Advances and Future Challenges, IEEE Trans. Nucl. Sci. 60 (2013) 2015-2036.

[8] G.L.M. Williams, E.J. Friebele, Space radiation effects on erbium-doped fiber devices: sources, amplifiers, and passive measurements, IEEE Trans. Nucl. Sci. 45 (1998) 1531-1536.

[9] S. Girard, B. Tortech, E. Regnier, M. Van Uffelen, A. Gusarov, Y. Ouerdane, J. Baggio, P. Paillet, V. Ferlet-Cavrois, A. Boukenter, J.P. Meunier, F. Berghmans, J.R. chwank, M.R. Shaneyfelt, J.A. Felix, E.W. Blackmore, H. Thienpont, Proton- and Gamma-Induced Effects on Erbium-Doped Optical Fibers, IEEE Trans. Nucl. Sci. 54 (2007) 2426-2434.

[10] P.L. Chu, Nonlinear effects in rare-earth-doped fibers and waveguides, IEEE LEOS, 1 (1997) 371-372.

[11] E.J. Friebele, Radiation protection of fiber optic materials: Effect of cerium doping on the radiation-induced absorption, Appl. Phys. Lett. 27(1975) 210-212.

[12] L.A. Tomashuk, K.M. Golant, Radiation-resistant and radiation-sensitive silica optical fibers, SPIE. 4083 (2000) 188.

[13] J. Thomas, M. Myara, L. Troussellier, E. Burov, A. Pastouret, D. Boivin, Gilles. Mélin, O. Gilard, M. Sotom, P. Signoret, Radiation-resistant erbium-doped-nanoparticles optical fiber for space applications, Opt. Express. 20 (2012) 2435-2444.

[14] D. L. Griscom, E.J. Friebele, K.J. Long, J.W. Fleming, Fundamental defect centers in glass: Electron spin resonance and optical absorption studies of irradiated phosphorus-doped silica glass and optical fibers, J. Appl. Phys. 54 (1983) 3743-3762.

[15] V. Pukhkaya, P. Goldner, A. Ferrier, N. Ollier, Impact of rare earth element clusters on the excited state lifetime evolution under irradiation in oxide glasses, Opt. Express. 23 (2015) 3270-3281.

[16] A. Ladaci, S. Girard, L. Mescia, T. Robin, A. Laurent, B. Cadier, M. Boutillier, Y. Ouerdane, and A. Boukenter, Optimized radiation-hardened erbium doped fiber amplifiers for long space missions, J. Appl. Phys. 121 (2017) 163104.

[17] A. Ladaci, S. Girard, L. Mescia, T. Robin, A. Laurent, B. Cadier, M Boutillier, Y Ouerdane and A Boukenter, Optimization of rare-earth-doped amplifiers for space mission through a

hardening-by-system strategy, Proc. SPIE 10096, Free-Space Laser Communication and Atmospheric Propagation XXIX, 100960F (February 24, 2017).

[18] S. Girard et al., Design of Radiation-Hardened Rare-Earth Doped Amplifiers Through a Coupled Experiment/Simulation Approach, in J. Lightw. Technol. 31(2013) 1247-1254.

[19] O. Berne, M. Caussanel and O. Gilard, A model for the prediction of EDFA gain in a space radiation environment, IEEE Photon. Technol. Lett. 16 (2004) 2227-2229.

[20] A. Ladaci, S. Girard, L. Mescia, T. Robin, A. Laurent, B. Cadier, M. Boutillier, Y. Ouerdane and A. Boukenter, Influence of Rare-Earth Ions Spectroscopic Parameters on Er-Yb Doped Fiber Amplifier Performances, submitted to J. Lightw. Technol. 2017.

[21] S. Girard, A. Laurent, E. Pinsard, T. Robin, B. Cadier, M. Boutillier, C. Marcandella, A. Boukenter, and Y. Ouerdane, Radiation-hard erbium optical fiber and fiber amplifier for both low- and high-dose space missions, Opt. Lett. 39(2014) 2541-2544.

[22] See http://www.photonics.ixblue.com/ for iXBlue Photonics, Specialty: fiber optics, bragg grating and optical modulation for communication, lasers, lidars and sensors.

[23] J. Linnros, N. Lalic, A. Galeckas, and V. Grivickas, Analysis of the stretched exponential photoluminescence decay from nanometer-sized silicon crystals in SiO_2, J. Appl. Phys. 86 (1999) 6128.

[24] E. Regnier, I. Flammer, S. Girard, F. Gooijer, F. Achten, G. Kuyt, Low-Dose Radiation-Induced Attenuation at InfraRed Wavelengths for P-Doped, Ge-Doped and Pure Silica-Core Optical Fibres, in Nuclear Science, IEEE Trans. Nucl. Sci , 54 (2007) 1115-1119.

[25] S. Girard, Y. Ouerdane, B. Tortech, C. Marcandella, T. Robin, B. Cadier, J. Baggio, P. Paillet, V. Ferlet-Cavrois, A. Boukenter, J.P. Meunier, J.R. Schwank, M.R. Shaneyfelt, P.E. Dodd, E.W. Blackmore, Radiation Effects on Ytterbium- and Ytterbium/Erbium-Doped Double-Clad Optical Fibers, IEEE Trans. Nucl. Sci. 56 (2009) 3293-3299.

[26] M. Vivona, S. Girard, T. Robin, B. Cadier, L. Vaccaro, M. Cannas, A. Boukenter, Y. Ouerdane, Influence of Ce^{3+} Codoping on the Photoluminescence Excitation Channels of Phosphosilicate Yb/Er-Doped Glasses, IEEE Photon. Technol. Lett. 24 (2012) 509-511.

[27] S. Girard, M. Vivona, A. Laurent, B. Cadier, C. Marcandella, T. Robin, E. Pinsard, A. Boukenter, Y. Ouerdane, Radiation hardening techniques for Er/Yb doped optical fibers and amplifiers for space application, Opt. Express. 20 (2012) 8457-8465.

[28] H. Henschel, O. Kohn, Regeneration of irradiated optical fibres by photobleaching, IEEE Trans. Nucl. Sci. 47 (2000) 699–704.

[29] S, Agnello, Gamma ray induced processes of point defect conversion in silica, PhD thesis Palermo, December 2000. http://www1.unipa.it/lamp/AgnelloPhDThesis.pdf.

[30] S. Girard, J. Keurinck, Y. Ouerdane, J.P. Meunier, A. Boukenter, J.L. Derep, B. Azais, P. Charre, M. Vie, Pulsed X-ray and γ rays irradiation effects on polarization-maintaining optical fibers, IEEE Trans. Nucl. Sci. 51 (2004) 2740-2746.

[31] Y.G. Choi K.H. Kim, Comparative study of energy transfers from Er^{3+} to Ce^{3+} in tellurite and sulfide glasses under 980 nm excitation, J. Appl. Phys. 88 (2000) 3832.